Electrical Retention of Optically Recovered Current in Back-Junction Silicon Heterojunction Solar Cells with Nanocrystalline Hole Contacts

Phillip Harris Paul[1,*] and Andrew Martin[1]

[1] Lawrence Livermore National Laboratory, 7000 East Avenue, Livermore, California 94550
* Correspondence: paul_harris@gse.harvard.edu

Abstract: Back-junction SHJ cells benefit from superb crystalline-silicon passivation while being subjected to challenging demands on doped-silicon carrier transport, transparent-conductive-oxide (TCO) conductivity and rear optical design. The key question studied here is to what extent the increase in photocurrent due to optical improvements is maintained in power output after the rear hole-selective contact replacement from p-a-Si:H to p-nc-Si:H. The comparison between four particular cells is used: a 25.26 % p-a-Si:H contact cell, a 26.30 % p-nc-Si:H cell with 86.59 % fill factor, a 26.74 % front-optics cell with $J_{SC} = 41.16\,mA\,cm^{-2}$, and a 26.81 % MgF_2/Ag rear-stack cell with $V_{OC} = 751.4\,mV$, $J_{SC} = 41.45\,mA\,cm^{-2}$ and FF = 86.07 %. The transition from 25.26 % to 26.81 % efficiency is associated with an 2.9 mV increase in open-circuit voltage, an $1.97\,mA\,cm^{-2}$ rise in current density and an 0.57 % fill-factor improvement. The p-nc-Si:H rear-contact decreases the series resistance from $381\,m\Omega\,cm^2$ to $206\,m\Omega\,cm^2$ and minimizes the rear HSC power loss from $0.41\,mW\,cm^{-2}$ to $0.13\,mW\,cm^{-2}$. The latter optical step increases the current density by $0.29\,mA\,cm^{-2}$ but produces only 0.07 percentage points gain in efficiency, which proves that rear-stack increase in the current density is offset in part by the fill-factor dependence on TCO conductivity. In terms of device physics, this means that there is a retained current scenario: contact loss reduction makes the fill-factor high, optical optimizations of the front side are responsible for the major part of the current-density increase and the rear reflector contribution at the last step is limited by the current retention.

Keywords: silicon heterojunction solar cell; nanocrystalline silicon; hole-selective contact; transparent conductive oxide; contact resistivity; fill factor; optical loss; current retention

Citation: Phillip Harris Paul and Andrew Martin. 2023. Electrical Retention of Optically Recovered Current in Back-Junction Silicon Heterojunction Solar Cells with Nanocrystalline Hole Contacts. *TK Techforum Journal (ThyssenKrupp Techforum)* 2023(3): 18–34.

Received: May-24-2023
Accepted: December-17-2023
Published: December-30-2023

1. Introduction

Photovoltaic devices based on crystalline silicon have progressed into a period where efficiency improvements rely more heavily on the combined control of carrier-selective contacts, parasitic absorption, transport, and lateral metalization losses than absorber properties alone [1]. The common trait of high-efficiency PERC, tunnel-oxide passivated contact, poly-Si-on-oxide, interdigitated back contact and SHJ cells is low surface recombination during movement of majority carriers through the contact structure with minimum losses. High-efficiency cells exhibit such strong coupling between contact and efficiency that an increase of current density can decrease terminal power if it is accompanied by a decrease of fill factor and an extraction barrier [2].

High-efficiency SHJ cells provide a good illustration of the phenomenon. The intrinsic hydrogenated amorphous silicon film passivates the surface of crystalline silicon substrate, the doped hydrogenated silicon provides carrier selectivity, while the TCO layers conduct currents and allow light penetration into the substrate [3,4]. Simultaneously, these films can absorb light, increase transport losses and create interfacial barriers due to inadequate doped-silicon/TCO interface design [5,6]. Consequently, a terminal efficiency above 26 % has to be interpreted in terms of three terminal parameters together: the open-circuit

voltage (V_{OC}) represents the level of surface passivation, the short-circuit current density (J_{SC}) is determined by the optical access and carrier collection, and FF shows whether the contact structure is capable of producing useful power out of the photogenerated current [7–9].

The use of p-nc-Si:H as hole contact is crucial in the context. Nanocrystalline and microcrystalline doped-silicon films have the potential to increase transport selectivity and improve conductivity in comparison with p-a-Si:H, but it is not always true as crystallization effects, incubation behavior, interfacial damage, and TCO compatibility can deteriorate both the passivation quality and contact selectivity [10–12]. An efficient p-nc-Si:H contact should thus meet two criteria: it should minimize hole-extraction resistance and maintain low recombination current responsible for V_{OC} [13–15].

Recent SHJ records demonstrate the need of such a combined interpretation of efficiency improvements. The 26.81 % back-junction SHJ cell with electrically optimized nanocrystalline-silicon hole contacts showed that low contact resistivity, TCO compatibility and optical improvement can be achieved in one industrial wafer [16]. Back-contact cells with heterojunction configuration have already reached efficiencies above 27 % by optimizing laser patterning, rear contact layout, anti-reflection coatings and edge passivation [17,18]. The results on industrial-size wafer and module level provide another condition: the high FF value has to be kept throughout interconnection, encapsulation and metallization [19]. The modern SHJ literature thus treats passivating selective contacts, TCO design and light management as one electrical-optical system, not as separate fabrication stages [20].

Light management brings a second aspect into the consideration. Escape of light from the front side, shading, front reflection, TCO absorption, window-layer absorption and rear reflection define J_{SC} [21]. At the same time, higher J_{SC} does not necessarily result in better cell performance due to lower TCO conductivity, sheet resistance, contact resistivity or transport selectivity [22,23]. The important issue is thus not only how many additional photons can be collected, but how much of this increased current remains in the form of terminal efficiency after subtracting FF and voltage penalties [24].

The article poses a precise device physics question: in the transition from a 25.26 % p-a-Si:H contact cell to a 26.81 % p-nc-SI:H back-junction SHJ cell, what part of the stack is responsible for conversion of additional current into terminal efficiency? The answer will be obtained by separating the terminal values of the cell parameters, the contact-transport quantities and the light-loss quantities, which are numerically available for the SHJ sequence. Such separation is necessary to avoid the creation of artificial cell rows using numbers belonging to different devices and to get an interpretation specific to the changes in contact and optics.

This separation is needed because of the modern stage of crystalline-silicon photovoltaic development. Terminal efficiencies of practical cells approach the limit of single-junction silicon cells, and large efficiency gains seldom occur from one physical effect alone. The limiting trade-off is defined by a product of several small quantities: a few millivolts of V_{OC}, a fraction of percentage point in FF, a few tenths of a mA cm^{-2} in J_{SC} and a contact loss that might be small in absolute power density, but becomes critical due to operation at high currents. The recombination limits in crystalline silicon and the reassessment of Auger recombination show that improvement of voltage is becoming increasingly costly as surface passivation approaches its highest value [25]. In such a regime, the optical and contact parts of the cell have to be considered in combination as the product law in Eq. (1) can amplify or cancel each individual change.

The previous development of SHJ solar cells revealed the importance of the intrinsic a-Si:H passivation layer. This layer provides high surface passivation while avoiding high-temperature dopant diffusion, and this was the reason for the achievement of high voltage in relatively thin crystalline-silicon wafers by HIT and SHJ cells [3]. The subsequent switch to back-contact and back-junction designs has led to the removal of restrictions imposed by front metal contacts and made it possible to optimize the illuminated side for light access

[5]. These advantages, however, shift a greater responsibility to the rear contact stack. The rear side has to collect carriers, provide selectivity, support lateral or local extraction and reflect light. An inadequate contact stack, thus, can make an optically optimized cell look underperforming.

The p-a-Si:H hole contact is thus a useful but flawed solution to this problem. While it behaves well as a passivating contact and allows for high values of V_{OC}, its poor conductivity and somewhat adverse transport barrier can penalize fill factor when current density increases. Studies of doped amorphous-silicon emitters and TCO/doped-silicon interfaces have shown that the transport penalty is related not only to the sheet resistance of the interface; the factors involved include band alignment, interfacial oxides, contact resistivity and carrier tunneling across the doped-silicon/TCO junction [7]. The p-nc-Si:H contact with its enhanced conductivity and reduced activation energy is desirable, provided that it does not damage the passivated interface [10,13].

Optical performance enhancements in SHJ cells also share the same coupled character. While a thinner front stack would provide more entry of photons into the structure, it is also the TCO layer that transmits the light which conducts current. Less metallization helps decrease shading, but can introduce extra lateral resistance if finger layout and TCO conductance do not match up. Reflection from the rear side would help recycle long-wavelength photons back into the absorber layer, but both TCO and metal reflectors are also part of the electrical stack. The classical explanation for light-trapping in the case of silicon gives us reason to take into account the importance of internal optical path length and angular redistribution [21]; in practical SHJ cases, however, we also need to consider the current-equivalent losses that arise from transparent layers, doped windows and electrodes [22–24].

This is why the current manuscript treats the 26.81 % SHJ cell as a succession of coupled states of operation rather than just an efficiency figure. The highest efficiency is, of course, the goal, but the main evidence here is the process that leads to this result. The p-nc-Si:H hole contact first decreases the electrical penalty from the rear side. Then the front side modifications help increase the current. Finally, the introduction of the MgF_2/Ag rear stack and TCO transmittance optimization provide an additional boost of current, although the efficiency gain is less pronounced due to fill factor sensitivity. Thus, the interpretation of this particular SHJ cell is done based on the preservation of current gain in terms of power generation, rather than just on the observation of current gain alone.

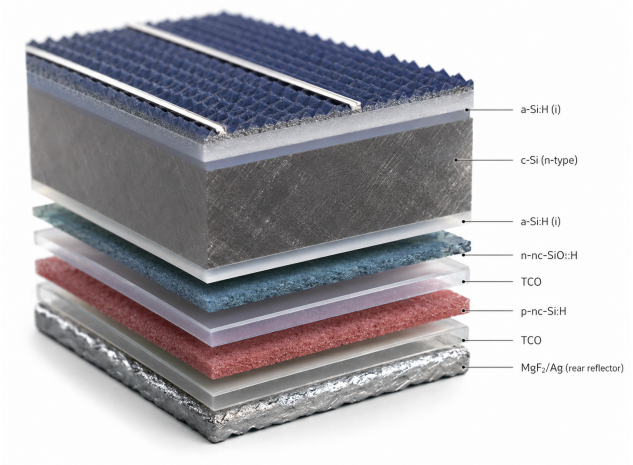

Figure 1. Back-junction SHJ stack.

The layered device structure of Figure 1 sets the terminology used throughout this manuscript. The c-Si absorber is surrounded by intrinsic a-Si:H passivation and carrier-selective layers, whereas the rear side comprises the contact-optical stack p-nc-Si:H/TCO/Mg F_2/Ag which helps decide whether the additional current can be extracted without FF loss.

2. Cell quantities and calculation procedure

The four cell levels make up the numerical background for the analysis: the 25.26 % p-a-Si:H contact cell, the 26.30 % p-nc-Si:H cell with 86.59 % FF, the 26.74 % front-optics cell and the 26.81 % rear-stack cell [16]. The last cell is defined by $V_{OC} = 751.4\,\text{mV}$, $J_{SC} = 41.45\,\text{mA cm}^{-2}$ and FF = 86.07 %. The transition from the p-a-Si:H contact cell to the last one includes an increase in the values of V_{OC}, J_{SC} and FF by 2.9 mV, 1.97 mA cm^{-2} and approximately 0.57 %, correspondingly.

The numerical sequence in Table 1 is purposely conservative. In case of the high-FF p-nc-Si:H cell, the electrical properties of the contacts system are defined, and in case of the rear-stack cell, the highest PCE and current density values are determined. These two cell types cannot be combined in one line, except when the variables are the same for the same cell type. This is necessary because otherwise the analysis of the high-efficiency SHJ cells may overestimate the availability of maximum voltage, current and FF at the same time.

Camera sequence of states in Figure 2 transforms Table 1 to the corresponding sequence used in the calculations. The first and last cell provide complete range of terminal motion, front-optics and rear-stack states provide the final current retention step, while high-FF p-nc-Si:H cell state provides the contact configuration that allows current gain due to optics without loss of FF at once.

Table 1. Cell quantities.

Cell level	Contact or optical condition	Numerical quantities used	Permitted calculation
p-a-Si:H contact cell	Amorphous p-type rear hole contact	PCE 25.26 %; $J_{SC} = 39.48\,\text{mA cm}^{-2}$; V_{OC} lower by 2.9 mV; FF lower by 0.57 % absolute	Terminal-variable change
p-nc-Si:H high-FF cell	Nanocrystalline p-type hole contact with optimized TCO coupling	PCE 26.30 %; FF 86.59 %	Contact-enabled FF
front-optics cell	Reduced front metal fraction and modified window stack	PCE 26.74 %; $J_{SC} = 41.16\,\text{mA cm}^{-2}$	Optical current step
MgF_2/Ag rear-stack cell	Higher rear reflection and adjusted TCO transmittance	PCE 26.81 %; $V_{OC} = 751.4\,\text{mV}$; $J_{SC} = 41.45\,\text{mA cm}^{-2}$; FF 86.07 %	Final current retention

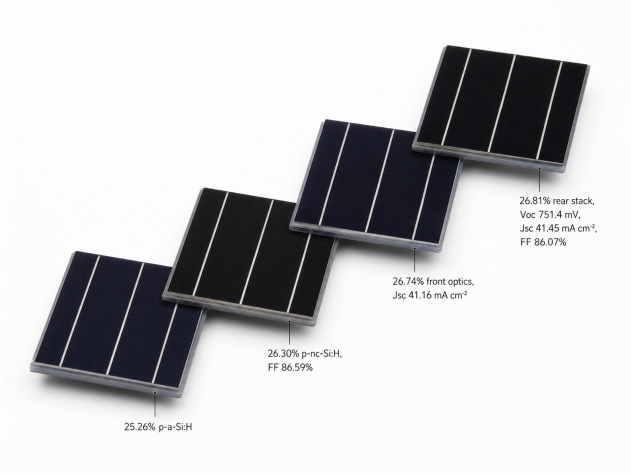

Figure 2. Cell-state sequence.

The terminal conversion efficiency is defined as

$$\eta = \frac{V_{OC} J_{SC} \text{FF}}{P_{in}}, \tag{1}$$

where V_{OC} is in volts, J_{SC} is in current-density units, FF is a fractional value and $P_{in} = 100\,\text{mW cm}^{-2}$. The relative change in a terminal quantity X between the p-a-Si:H contact cell and the final cell is calculated as

$$\Delta X_{rel} = \frac{X_{26.81} - X_{25.26}}{X_{25.26}} \times 100\%. \tag{2}$$

A current-retention coefficient is then used for cell pairs where both PCE and J_{SC} are specified:

$$\Gamma = \frac{\Delta\eta}{\Delta J_{SC}}. \tag{3}$$

The coefficient Γ is not considered to be a universal material constant. The coefficient is the cell-level coefficient showing how many efficiency percentage points have been gained with each new $\mathrm{mA\,cm^{-2}}$ on a specified transition.

The computation is intentionally limited to the quantities that can be attributed to a specified cell state. This has immediate implications for the interpretation of FF. While the 26.30 % p-nc-Si:H cell has the maximum stated FF of 86.59 %, the last 26.81 % rear-stack cell has the highest PCE and J_{SC}, but has a little bit smaller FF of 86.07 %. The discrepancy is not seen as contradictory. It shows that contact optimization and optical adjustment are not the same electrical states. High-FF cell confirms the ability of the p-nc-Si:H/TCO contact, while rear-stack cell proves the maximal terminal efficiency with an additional optical tuning. Thus, the two lines are to be used for different purposes.

The same principle is applied to V_{OC}. The final device has $V_{OC} = 751.4\,\mathrm{mV}$ and the whole voltage shift from the p-a-Si:H contact cell is equal to 2.9 mV. Therefore, the corresponding starting voltage value is equal to 748.5 mV in the terminal performance comparison. Additional voltage values are introduced for the intermediate p-nc-Si:H and front-optics states only if they are necessary for a direct comparison. The absence of a particular value is significant, since it prevents the fabrication of an artificial performance route and keeps the analysis consistent with the real cell-state sequence.

The retention coefficient Γ is needed, since the efficiency equation alone does not show if the optical current increase has been effectively utilized. The cell could gain current and lose FF at the same time, so the overall efficiency change would be small in such case. Since the ratio of the efficiency increment to the current-density increment for a particular transition gives Γ, the current step is placed on the terminal-power scale with its help. High value of the coefficient shows that the increased current is effectively retained by the electrical stack. Low value means that the optical gain is partially filtered by the FF decrease, voltage change or the sensitivity to the series resistance. The coefficient is not meant to replace the detailed J–V analysis, but to serve as a simple diagnostic tool for the reported SHJ sequence.

The contact quantities are analyzed in the same way. The series resistance, rear-HSC power loss and contact resistivity are not used for the full equivalent circuit, since the complete set of diode and shunt parameters is not known. Instead, the values are used to find the direction and magnitude of the rear-contact improvement. The transmission-line measurement theory shows why contact resistivity should be separated from the total series resistance: the first one corresponds to the local contact interface, while the second one includes the lateral transport, metallization, TCO sheet resistance and other resistive elements [26–28]. Thus, the reduction from more than $100\,\mathrm{m\Omega\,cm^2}$ to less than $5\,\mathrm{m\Omega\,cm^2}$ is taken as a strong evidence that the p-nc-Si:H/TCO interface is not the dominant current extraction barrier anymore.

The figures are used as analytical tools rather than decorative summaries. The architecture view shows the physical layer sequence, the state sequence highlights the devices that can be compared, the terminal matrix illustrates the behavior of the performance variables, the rear-contact picture compares the electrical bottleneck, the optical-loss landscape pinpoints the remaining current reserve, the retention plane quantifies the current-to-efficiency conversion and the final design-rule picture summarizes the sequence in engineering priorities. Each visual element is connected to the table or numerical comparison, so the figure discussion is supported by the same data that were used in the computations.

3. Results and discussion

3.1. Movement of the terminal variables from p-a-Si:H to p-nc-Si:H SHJ

The 25.26 % to 26.81 % move results in an increase in the PCE by 1.55 percentage points, which translates to an increase of about 6.14 % relative to the former. The current-density increase is 1.97 mA cm^{-2}, while the voltage increase is relatively small at just 2.9 mV. While the FF variation is moderate in absolute value, it is very important because the current variation of around 41 mA cm^{-2} can only result in low terminal power without increasing the FF of the transport stack.

From Table 2, one learns that the high-efficiency cell is not voltage-led. The voltage is already nearly saturated for such an SHJ structure. The most prominent numeric change is in J_{SC}. The fill-factor increase appears quite low when viewed as a percentage change, but in a high current density case, it amounts to the difference between optical and useful electrical power. Thus, the device needs both more photon-generated current and a contact stack that ensures FF > 86 %.

Table 2. Terminal quantities.

Quantity	p-a-Si:H contact cell	final rear-stack cell	Change
PCE	25.26 %	26.81 %	+1.55 percentage points
V_{OC}	748.5 mV	751.4 mV	+2.9 mV
J_{SC}	39.48 mA cm^{-2}	41.45 mA cm^{-2}	+1.97 mA cm^{-2}
FF	85.50 %	86.07 %	+0.57 % absolute

In particular, Figure 3 highlights the fact that the changes in the terminal variables occur very unequally. PCE and J_{SC} improve noticeably from the first to the final cell state, whereas V_{OC} changes by just 2.9 mV. Figure 3 explains why the 86.59 % FF value in the p-nc-Si:H state is significant although not the final record cell since it proves the possibility of operation with high FF at the intermediate stage after the contact replacement but before the final rear-stack optical adjustment.

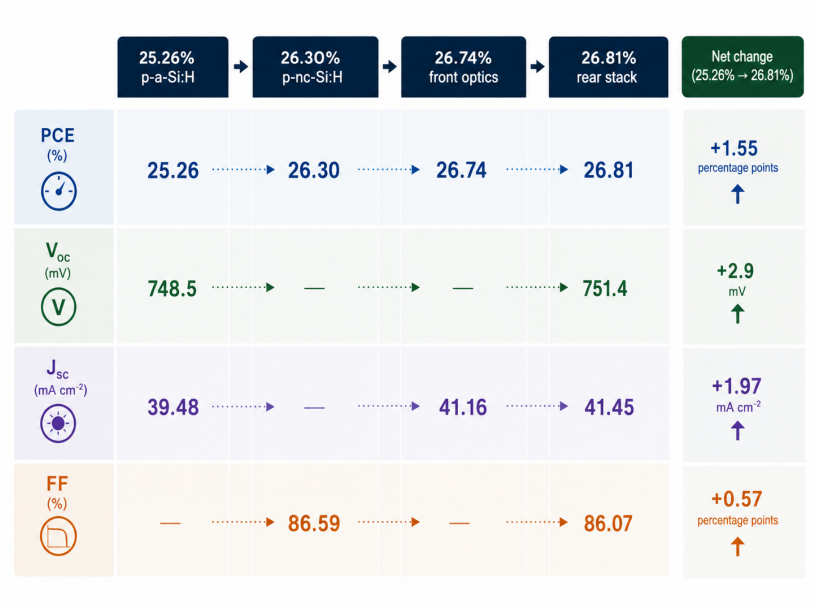

Figure 3. Terminal progression.

Besides, the terminal matrix is convenient due to separating absolute and relative importance. The voltage gain by 2.9 mV is good, but it is not large enough to be responsible for a 1.55 percentage-point efficiency increase. At the same time, the increase in J_{SC} by 1.97 mA cm^{-2} is sufficiently large to dominate the change in PCE provided FF is kept high enough. This kind of behavior corresponds to a good passivated SHJ device, where voltage

is already very high for a crystalline-silicon absorber with thin intrinsic a-Si:H passivation [3,6]. In this case, the device does not need a large voltage correction; what it needs is a contact stack that allows the additional current to stay electrically useful.

The second observation comes from the FF row. The final FF of 86.07 % is less than the 86.59 % value obtained for the p-nc-Si:H high-FF cell, but it is still higher than the FF at the p-a-Si:H contact condition by about 0.57 % absolute. It means that the final device has two features simultaneously: the rear contact has significantly been improved compared to the p-a-Si:H condition, but the last optical adjustment has made the FF sensitivity reappear. The correct interpretation in this case is thus not that the final cell has the best value for each parameter, but it has the best compromise between current, voltage and FF after all the optical and electrical corrections have been applied.

The high-FF intermediate state is important because it shows how the rear contact itself operates. An intermediate cell with p-nc-Si:H contact, PCE = 26.30 % and FF = 86.59 % shows that the contact material is capable of providing excellent extraction provided that the surrounding TCO and optical conditions are adequate. The next movement up to 26.81 % efficiency uses more current, but at a bit smaller FF. This is the key point in the paper since the final efficiency is the highest, but the last current increment is not fully retained as efficiency. That is, the record cell results from a balance, not from a continuous improvement in all terminal variables.

Finally, the terminal quantities shown in Figure 3 warn that when making comparisons between the reported high-efficiency SHJ devices, one should be careful with just looking at the single PCE number. Two cells can differ by a few tenths of a percentage point in efficiency and be governed by different bottlenecks. For the present progression, the large change in J_{SC} and small change in V_{OC} indicate the main trend of improvement, while the FF row indicates the condition of retention of this improvement.

3.2. Rear hole-contact transport as the electrical release step

The most drastic changes in terms of mechanisms happen at the rear hole-selective contact. The p-nc-Si:H material features the crystallinity above 63 %, conductivity above $3\,S\,cm^{-1}$, activation energy below 115 meV and a conductivity advantage of over four orders of magnitude in relation to standard p-a-Si:H layers [16]. On the cell level, the series resistance decreases from $381\,m\Omega\,cm^2$ to $206\,m\Omega\,cm^2$, and the power loss due to the rear HSC decreases from $0.41\,mW\,cm^{-2}$ to $0.13\,mW\,cm^{-2}$. It can be concluded from these figures that the p-nc-Si:H/TCO interface is the electrical release point, which comes before the gain steps.

From Table 3, one sees why it is impossible to view the p-nc-Si:H layer as an optical tuning layer or an equivalent contact-replacement layer. Its primary function is removing an electrical bottleneck, at the same time preserving the passivation environment, which is necessary for achieving high V_{OC}. This approach fits perfectly into the concept of the contact-selectivity theory, where efficient passivation contact requires not only low recombination but also low majority-carrier resistance [29]. Furthermore, it is consistent with the transport study of SHJ structures, where TCO/doped-silicon interfaces define the usable FF even if c-Si/a-Si:H interface is well-passivated [8,9].

Table 3. Contact transport.

Quantity	p-a-Si:H contact condition	p-nc-Si:H contact condition	Electrical meaning
Crystallinity	amorphous p-layer	$> 63\,\%$	conductive nanocrystalline network
Conductivity	lower by more than four orders of magnitude	$> 3\,S\,cm^{-1}$	stronger hole transport
Activation energy	higher p-layer transport barrier	$< 115\,meV$	reduced extraction barrier
Total series resistance	$381\,m\Omega\,cm^2$	$206\,m\Omega\,cm^2$	lower resistive loss
Rear-HSC power loss	$0.41\,mW\,cm^{-2}$	$0.13\,mW\,cm^{-2}$	reduced rear-contact penalty
Contact resistivity	$> 100\,m\Omega\,cm^2$ before optimization	$< 5\,m\Omega\,cm^2$ after optimization	low-resistance TCO contact

Paired rear contacts of Figure 4 help us to represent the difference between two SHJ rear-hole contacts from the point of view of their transport parameters. The p-a-Si:H case has larger series resistance, higher rear-HSC power loss and higher contact resistivity, while the p-nc-Si:H case has lower series resistance, larger p-layer conductivity and smaller

activation barrier. This means that using the nanocrystalline rear contact leads to changing the boundary conditions for any further optical improvement: extra current may be utilized only if the extraction penalty of the rear contact is lowered.

Contact optimization in Figure 4 is physically significant, since SHJ cells often have excellent passivation before they have good extraction. Although the intrinsic a-Si:H layer has good interface passivation properties, doped layer with poor conductivity or unfavorable interface with the TCO layer can lead to lowering of FF even if the c-Si/a-Si:H interface is well-passivated. The solution of this problem is achieved through the use of more conductive mixed-phase material. Conductivity above $3\,\mathrm{S\,cm^{-1}}$ and crystallinity above 63 % show that the layer is not only slightly modified amorphous film. It has transport properties that allow holes to move easier through the rear contact with preserving the passivating stack.

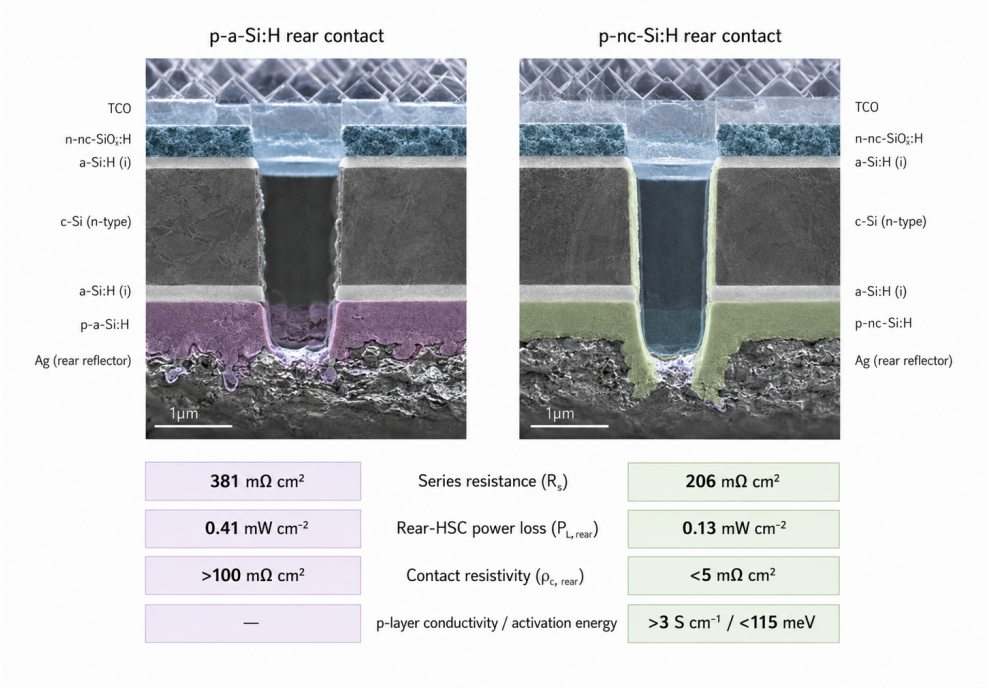

Figure 4. Rear-contact comparison.

Small value of the activation energy below 115 meV confirms this conclusion from another point of view. Lower activation energy means that carrier transport through the doped layer needs smaller thermal barrier. This fact is important, since series resistance is not always determined only by metal geometry. In SHJ cells, doped-silicon/TCO interface may act as a selective but resistive junction, and small interfacial oxides or band offsets may change the behavior of the contact [8]. Thus, p-nc-Si:H/TCO contact is the result of interface engineering as well as a material one.

The scale of the resistance change is big enough to have influence on FF at device level. Series resistance is decreased from $381\,\mathrm{m\Omega\,cm^2}$ to $206\,\mathrm{m\Omega\,cm^2}$. It is not a small correction: it eliminates about $175\,\mathrm{m\Omega\,cm^2}$ from the resistive path. It means that at current densities above $40\,\mathrm{mA\,cm^{-2}}$, this change will affect directly the shape of the J–V curve near the maximum-power point. Corresponding change of the rear-HSC power loss from $0.41\,\mathrm{mW\,cm^{-2}}$ to $0.13\,\mathrm{mW\,cm^{-2}}$ shows the same result, but in terms of power density units: the rear contact losses less of the power generated by the optical stack.

Contact resistivity change is more indicative. Local contact resistivity above $100\,\mathrm{m\Omega\,cm^2}$ may become serious penalty in a back-junction structure because the rear side must collect carriers through a locally contacted or patterned stack. The reduction of this value below $5\,\mathrm{m\Omega\,cm^2}$ makes the contact move to the range required for high-current applications. Standard contact analysis methods stress the fact that measured resistance depends on both

contact geometry and sheet transport [26,27]. Therefore, the current comparison should be viewed as combined improvement of the p-nc-Si:H layer, its interface with TCO and the rear extraction channel, not as isolated film property.

Contact interpretation above also explains why the increase in voltage is small. If there was new hole contact with high interface recombination, then the final voltage would be reduced and/or unstable. But there is not such case: it has high voltage and additional 2.9 mV. Thus, the improvement has signatures of better selectivity: the majority-carrier extraction is enhanced and minority-carrier recombination is under control. This situation corresponds to the concept of the passivating contact, where low recombination and low majority-carrier resistance must exist together [29].

3.3. Current recovery through optics and maintaining fill-factor

Following electrical optimization of the rear contact, further front side optical optimization increases the current density to $J_{SC} = 41.16\,\mathrm{mA\,cm^{-2}}$ at 26.74 % PCE. The final MgF_2/Ag rear stack and the TCO-transmittance modification leads to an increase in J_{SC} to $41.45\,\mathrm{mA\,cm^{-2}}$. In the final step, the improvement in efficiency is just 0.07 percentage point since the fill factor decreases due to a modified TCO condition [16]. The final current density is thus a real current, but its conversion to terminal power is not complete.

The optical losses in Table 4 demonstrate that further increases in current gain are physically possible but electrically unavailable. Front escape remains the dominant current-equivalent loss term, and both losses from shading and from absorption of TCOs are high enough to be significant in a 26 %-level SHJ cell. Such losses demonstrate why no gains can be expected from purely optical thickening or improved reflectance in the future. Any optical enhancement should leave contact and conductive-oxide current pathways able to ensure FF.

Table 4. Optical current losses.

Loss term	Current-equivalent loss	Device interpretation
Front escape	$2.43\,\mathrm{mA\,cm^{-2}}$	Largest current reserve, governed by texture, angular response and front-stack optics
Electrode shading	$0.97\,\mathrm{mA\,cm^{-2}}$	Metallization remains a substantial loss even after front metal reduction
Front TCO absorption	$0.50\,\mathrm{mA\,cm^{-2}}$	TCO transparency and sheet conductance must be optimized together
i-a-Si:H absorption	$0.34\,\mathrm{mA\,cm^{-2}}$	Passivation layers retain a measurable optical cost
Front reflection	$0.27\,\mathrm{mA\,cm^{-2}}$	Smaller than escape loss but relevant at high current density
Rear TCO absorption	$0.25\,\mathrm{mA\,cm^{-2}}$	Rear optical gain is coupled to conductive-oxide absorption
n-nc-SiO_x:H absorption	$0.21\,\mathrm{mA\,cm^{-2}}$	Front selective/window layer still contributes to current loss
Test-chuck loss	$0.12\,\mathrm{mA\,cm^{-2}}$	Small contribution relative to front escape, shading and TCO absorption

The optical loss landscape in Figure 5 illustrates the spatial nature of the current-equivalent losses. Front escape remains the highest branch, shading remains the second one, and losses from TCO absorption, window and passivation absorption compose the medium branch with lesser but still significant losses. As the addition in the rear stack step brings only $0.29\,\mathrm{mA\,cm^{-2}}$ current, even relatively small increase in conductance or contact losses in the transparent conductive oxide can absorb a considerable part of the optical gain.

The optical loss distribution demonstrates that there is a substantial current potential in the cell even after reaching the 26.81 % efficiency level. The front escape remains the highest term equal to $2.43\,\mathrm{mA\,cm^{-2}}$. This value is higher than the entire current increase from the p-a-Si:H contact cell to the rear-stack cell. Therefore, front escape cannot be considered as the residual imperfection. It defines angular light management, front-texture engineering, refractive index matching and module interface optimizations as major

directions of improving the current generation ability, provided that these changes do not lead to increased recombination and lateral transport losses.

The second-largest optical loss in the table is electrode shading with a value of 0.97 mA cm^{-2}. In back junction devices, front side already provides less constraints than in front junction metallized devices, but the above figure demonstrates that the existing front electrodes have a non-negligible current cost. Reducing shading is not merely a question of shrinking the electrode dimensions, because the trade-off between resistive losses, contact geometry and module interconnections should be considered. The same principle explains why high-efficiency back contact SHJ cells are using the patterning and edge control instead of one optical modification [17,18].

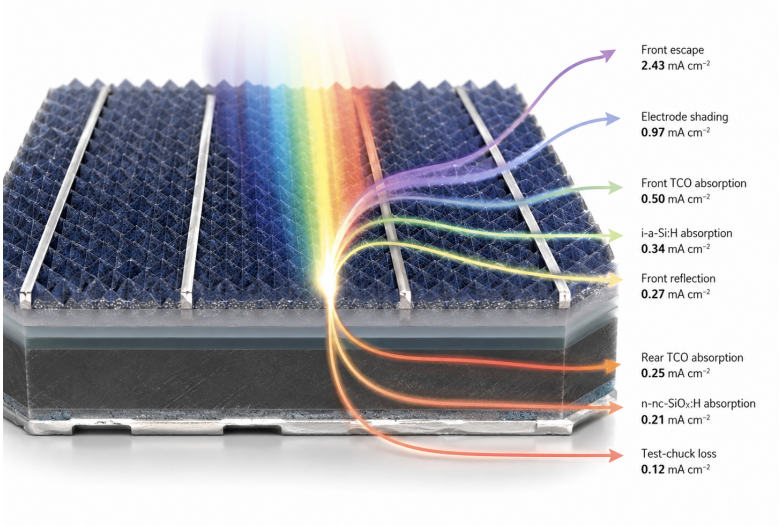

Figure 5. Optical-loss landscape.

The front TCO absorption with a value of 0.50 mA cm^{-2} is especially interesting in the context of the retention problem. More transparent TCO can increase J_{SC}, but changing unfavourable carrier density, mobility, thickness or sheet conductance will decrease FF. Such a trade-off is clearly seen in the rear stack step where J_{SC} increases from 41.16 mA cm^{-2} to 41.45 mA cm^{-2}, and PCE increases only by 0.07 percentage points. The optical current has been gained, but not all of it has been preserved due to the electrical constraints of the final stack structure.

The remaining absorption terms are individually smaller but are important collectively. Intrinsic a-Si:H absorption is 0.34 mA cm^{-2}; front reflection is 0.27 mA cm^{-2}; rear TCO absorption is 0.25 mA cm^{-2}; n-nc-SiO$_x$:H absorption is 0.21 mA cm^{-2}. These values are smaller than the front escape, but their sum exceeds the final current increment. It means that in the future cell, all losses should be taken into account even if their individual values are below one milliampere per square centimeter. Increments which are minor in the 26 %-level efficiency cell can define whether this cell can cross the next efficiency barrier.

The spatial visualization of losses in Figure 5 is intended to stress physical location. Losses at the front texture, metal grid, front TCO, passivation and rear stack are taking place at various depths along the same optical path. Hence, the ranking is not only numerical but spatial too. The design which is reducing front escape without increasing front TCO absorption is favourable, while the design which is reducing rear losses but is decreasing rear contact conductance can produce only a minor net gain. The proper optimization target thus cannot be maximum optical current itself. It should be the maximum optical current with preserved contact selectivity and FF.

The retention coefficient in Table 5 immediately resolves the question of how the introduced current is converted into the terminal efficiency. For the entire shift of 25.26 % to 26.81 %, every extra mA cm^{-2} of current amounts to 0.79 percentagepoints of extra efficiency. For the rear-stack shift, it becomes equal to 0.24.

Table 5. Current retention.

Transition	$\Delta\eta$ (pp)	ΔJ_{SC}	Γ	Interpretation
25.26 % to 26.81 %	+1.55	+1.97	0.79	Most of the current increase becomes useful because the contact loss is already reduced
26.74 % to 26.81 %	+0.07	+0.29	0.24	The final rear-stack current gain is partly filtered by FF reduction

Note: ΔJ_{SC} is given in mA cm^{-2}; Γ is expressed as PCE percentage points per mA cm^{-2}.

This dependency is illustrated in more detail on the phase plane in Figure 6. The entire shift of the device lies along a quite steep line passing through the origin because it involves both the release of contact and optical gain. In contrast, the rear-stack shift is positioned along a considerably less steep slope because here the gain of optical current is limited by the effect of the modified TCO on the FF factor. Therefore, this result represents very strong quantitative evidence that optical current cannot be studied separately from the contact transport.

The retention coefficients in Figure 6 allow quantifying this difference. In the shift of the whole device from 25.26 % to 26.81 %, $\Delta J_{SC} = 1.97\,\text{mA cm}^{-2}$ and $\Delta\eta = 1.55$ percentage points, hence $\Gamma = 0.79$. This coefficient is high due to the current gain being made after the major reduction of the rear contact penalty. In this case, the extra current is supplemented by a net FF increase rather than decrease, and the electric system of the cell is able to convert it effectively into the terminal power.

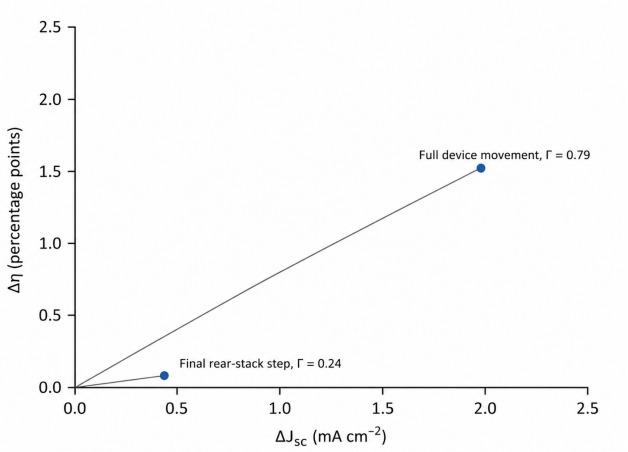

Figure 6. Current-retention plane.

The final shift of the rear stack demonstrates a different behavior. Here, the current gain of 0.29 mA cm^{-2} is true, but the PCE gain is only 0.07 percentage points, resulting in $\Gamma = 0.24$. This does not mean that the rear reflector is ineffective. Instead, it means that the marginal current gain achieved as the consequence of the rear MgF_2/Ag deposition and modification of the TCO transmittance is filtered by the existing electrical condition of the rear stack. Nevertheless, the highest PCE is achieved in the cell of this design, but the efficiency gain is lower compared to the whole movement.

This difference is crucial for evaluation of the high-efficiency achievement claims. The gain of the current density after the reduction of the contact penalty is usually associated with the high value of the terminal efficiency, while the same gain after worsening of the TCO conductivity is associated with a lower efficiency value. Therefore, the same current density increment is of different importance depending on its place in the cell design. The retention plane shows this dependency by translating the movement into the slope, rather than evaluating the current PCE and J_{SC} separately.

The coefficient also does not introduce too simplistic hierarchy in which the optics and contacts are considered as separate achievements. Indeed, the p-nc-Si:H contact does

not produce all of the optical current, while the optical stack does not generate all of the FF. The efficient device is the one in which these components work in the right sequence – first, the contact resistance is reduced, then the optical current is added at the stack capable of carrying it. When the optical modification starts affecting the TCO or contact conditions, the slope decreases. Therefore, the retention result provides the device-level answer to the research question.

3.4. Device-level interpretation

The p-nc-Si:H/TCO contact should be considered the key component that shifts the boundary of the SHJ cell operation. Instead of a simple addition to the rear stack conductivity, the contact allows all further optical current increases to be achieved in the high fill-factor mode. Such a conclusion arises from the joint optimization of the parameters of conductivity, activation energy, contact resistivity, series resistance and rear-HSC power loss. It is consistent with previous research that indicates the necessity of combined control of crystallinity and interfaces in doped nanocrystalline silicon to enable improvement in the SHJ cell performance [14,30,31].

The optical measurements suggest a second design rule. Improvements of front optics are very beneficial after contact losses are minimized, but the final rear-reflector optimization reveals that an optical current gain might be less critical for the PCE increase in case of a lower TCO conductivity. Therefore, conductive oxide is not a neutral layer of optics. It is a part of electrical contact and an optic component at the same time. The dual nature of TCO explains why the final current gain of 0.29 mA cm^{-2} contributes only 0.07 % of absolute efficiency gain.

The synthesis picture in Figure 7 summarizes the device interpretation in the form of priority list. Rear-contact transport release is the first condition, optical current harvesting is the second one and fill-factor preservation is the filter that decides whether the optical gain is effective for the final efficiency. In other words, the above list of design directions follows from the measurement quantities: minimize front escape, minimize shading, minimize TCO/window absorption and preserve low contact resistivity with low series resistance.

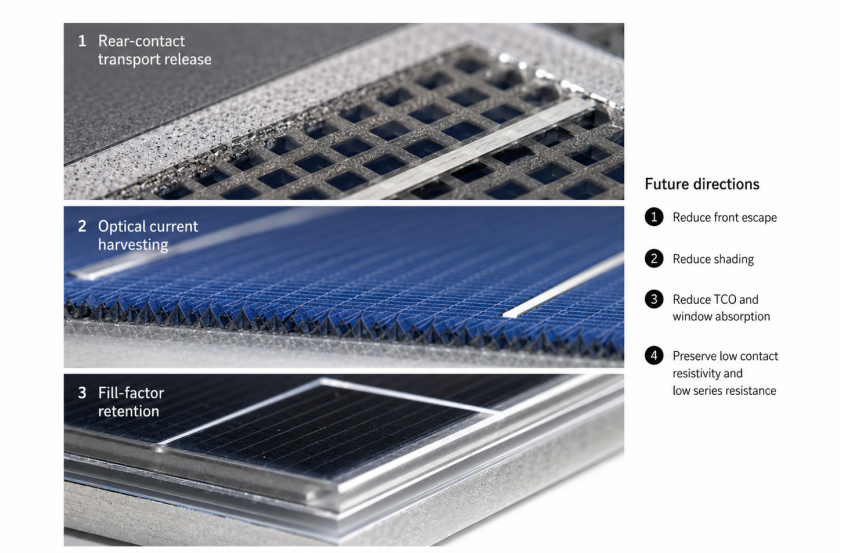

Figure 7. Design-rule synthesis.

The above synthesis in Figure 7 follows the interpretation discussed above. The first tier is the release of rear-contact transport. Without the reduction of contact resistivity, series resistance and rear-HSC power loss, the increased optical current would be much less effective. The second tier is the optical current harvesting. Front escape, shading and TCO/window absorption are still sufficient to achieve further current gains. The third tier is the FF preservation. Any optical change should be compared with the series resistance

and contact selectivity, since the final rear-stack optimization reveals how the increment of current results in the small increment of efficiency due to growing FF sensitivity.

The proposed design rule is consistent with the general trend of SHJ cells evolution. Reviews of passivating selective contacts highlight that the cell efficiency is determined by the selectivity rather than conductivity alone [2,20]. Publications on the production of p-type SHJ cells and cell-to-module ratios indicate that even laboratory-level improvement should survive scaling, metallization and module integration [19]. The current retention concept provides an additional perspective for solving the problem: the new process should be evaluated according to the fraction of the optical gain remaining in terminal power after considering all electrical penalties.

Some practical conclusions can be made. First, the further reduction of front escape should be performed with special care about the front TCO and window-layer stack since the major current reserve is located at the illuminated side. Second, the reduction of shading should be accompanied by the corresponding contact geometry in order to avoid cancellation of the increase in light entry due to lateral resistance. Third, the rear optics should be optimized along with the optimization of the conductive oxide to keep the rear p-nc-Si:H contact. Fourth, the current density gain should be reported in parallel with the values of FF, series resistance and contact resistivity since the current example proves that the sole J_{SC} can mislead about the device evolution.

The above analysis also explains the position of the final 26.81 % value. The device is not only an optical record and not only a contact record. It is a high-efficiency cell in which the electrical release makes the optical gain applicable. The rear p-nc-Si:H contact provides the high FF and the low rear loss; the front optical state provides the high current; the final rear stack provides the current but reveals the price of TCO-related FF retention. Such a combination of conditions makes the cell interesting from the scientific point of view since it demonstrates the sequence of constraints for future back-junction SHJ cells.

3.5. Implications for reporting high-current SHJ optimization

The current-retention result indicates that high-current SHJ optimization needs to be accompanied with more than just a final efficiency figure. The right report would describe at what cell level J_{SC} grows and at what level FF becomes maximum, and what contact/TCO conditions correspond to those two metrics. Without such separation, a reader may think that maximum current and maximum FF belong to one and the same cell. The present chain of steps shows how wrong this intuition can be. The 86.59 % FF corresponds to the p-nc-Si:H high-FF condition, while the 41.45 mA cm^{-2} current density corresponds to the rear-stack condition. Both parameters are important, but answer different questions.

Another implication related to reporting pertains to the use of optical-loss inventories. Current-equivalent losses are very helpful since they allow converting reflectance, absorption and shading into the unit of J_{SC}. This does not mean, however, that those currents can be added up to the final cell efficiency. Recovering 0.25 mA cm^{-2} from rear TCO absorption is valuable, but only if the TCO is conductive enough to provide FF. Similarly, recovering 0.50 mA cm^{-2} from front TCO absorption is constrained by sheet resistance and contact requirements. The optical inventory thus shows the opportunities, while the retention coefficient measures how effectively they are used.

The third implication is about scaling. Large-area cells and modules bring new resistive and optical constraints like interconnection resistance, metallization design, edge recombination, encapsulation optics and current mismatch. Recent efforts on transfer of high-efficiency SHJ cells into modules show the importance of the ratio between cell and module performance. The same reasoning holds at the cell scale, where the p-nc-Si:H contact, TCO and reflector define the retention coefficient before considering any module-level losses. Therefore, a good laboratory cell needs to be characterized with respect to both cell and module current retention.

Finally, there is a methodological implication. The retention coefficient is straightforward enough to be calculated based on the published PCE and J_{SC}, but sufficiently detailed

to reveal the loss of terminal effectiveness. It cannot substitute electrical modeling, Suns-V_{OC} analysis, contact resistivity measurements and optical simulations. However, it allows making the connection between the performance table and the physical structure chain. In the SHJ case presented above, this connection shows that the p-nc-Si:H rear contact allows high currents, while the final rear-stack increment in optical losses is restricted by FF retention.

3.6. Limitations of the interpretation and reproducibility

The interpretation stays within the limits of variables available for the four defined cell levels. It does not attempt to deduce a comprehensive parameter set of a dark diode, a complete recombination current splitting or an optical simulation. All of them would require spectra, complete illuminated and dark *J–V* curves, Suns-V_{OC} information, thickness of layers, mobility and concentration of carriers in TCO, information about metallization geometry and wafer resistivity. Instead, the paper poses the following narrower but relevant question: what restrictions do the terminal values and losses put on explaining the 26.81 % SHJ result? This limitation prevents the paper from attributing mechanisms to values which are not numerically justified.

At the same time, it preserves the function of the figures. Camera-type cell design and contact images are visual illustrations of the described layer structure and numeric comparison, not the substitution of the measurements. They illustrate the stack structure, show where the contact and optical modification come in and allow following the logic of the arguments. Quantitative data remain related only to the tables: terminal values, contact loss values, optical loss values and current retention coefficient. This distinction is crucial for scientific completeness since visual richness could hide the origin of the conclusion, whether numerical or interpretative.

The calculation can be reproduced using the table values. Full terminal movement involves 25.26 % and 26.81 % PCE values, 39.48 mA cm^{-2} and 41.45 mA cm^{-2} current density, the 2.9 mV voltage difference and approximate 0.57 % absolute FF increase. Final current retention movement involves 26.74 % front-optics state and 26.81 % rear-stack state. Using these values, the full transition produces $\Gamma = 1.55/1.97 = 0.79$, and the final transition produces $\Gamma = 0.07/0.29 = 0.24$. These two values are not fitting parameters; they are ratios that show how much each current increment contributes to the terminal efficiency.

Thus, the reproducibility criterion of the analysis is clearly stated. Each reader can take any other SHJ sequence and perform the same calculation, provided the compared states remain separated and PCE and J_{SC} are available for each transition. The value of the coefficient will vary depending on the cell design, TCO quality, contact stack and optical path, but the diagnostics remains the same. Large value of Γ means that the current gain is efficiently retained; the small one means that a certain part of the electrical stack filters the current gain before it appears as the efficiency.

Such an approach proves to be particularly helpful when evaluating high-efficiency silicon cells since there are many advances that happen on the sub-percentage level. A shift of 0.07 % of absolute PCE could still have a significant meaning when it happens at 27 % efficiency level, although the same shift could mean quite different physics depending on whether it was caused by voltage, current or FF. Placing the last rear-stack step against the full device movement allows revealing the meaning of a small PCE increment as the current gain with low retention.

4. Conclusion

The key research question answered in this manuscript concerns how much of the photocurrent recovered via optical refinements is kept as terminal efficiency when a back-junction SHJ solar cell is changed from a p-a-Si:H rear hole contact to a p-nc-Si:H rear hole contact and then moved to a high-current rear-stack condition. The result is a quantitative and sequential answer. Overall, the cell increases its efficiency from 25.26 % to 26.81 % by gaining 1.97 mA cm^{-2} in J_{SC}, 2.9 mV in V_{OC} and 0.57 % in FF. So, the 1.55 percentage points

efficiency increase is mostly due to current recovery, yet that current is retained since the rear contact provides an efficient electrical extraction channel.

The p-nc-Si:H/TCO rear contact is the essential electrical release condition. It brings total series resistance from 381 $m\Omega\,cm^2$ to 206 $m\Omega\,cm^2$, rear-HSC power dissipation from 0.41 $mW\,cm^{-2}$ to 0.13 $mW\,cm^{-2}$ and rear contact resistivity from above 100 $m\Omega\,cm^2$ to under 5 $m\Omega\,cm^2$. Thus, the contact condition change goes beyond mere structural substitution. It changes the electrical condition of the back-junction cell, providing the possibility to have high currents without voltage loss.

Optical refinement is equally specific. The front optical condition increases J_{SC} to 41.16 $mA\,cm^{-2}$, and the rear-stack condition combined with TCO transmittance optimization increases it to 41.45 $mA\,cm^{-2}$. The latter increase brings only 0.29 $mA\,cm^{-2}$ and 0.07 percentage points of PCE. Therefore, the current-retention coefficient drops from $\Gamma = 0.79$ for the entire device movement to $\Gamma = 0.24$ for the rear-stack condition. This is the key answer to the question raised in the manuscript: current is retained efficiently only if the contact and TCO conditions support FF.

Remaining current loss inventory identifies areas for efficiency improvements. Front escape is the largest current-equivalent loss equal to 2.43 $mA\,cm^{-2}$, followed by electrode shading (0.97 $mA\,cm^{-2}$) and front TCO absorption (0.50 $mA\,cm^{-2}$). It means that there is still optical potential for further efficiency increases, yet the current-retention result implies that this potential cannot be exploited automatically. All future current-gain steps should be accompanied by low contact resistivity, low series resistance and high FF.

Thus, the resulting design guideline is straightforward, yet strict. Back-junction SHJ optimization should start with establishing the p-nc-Si:H/TCO rear contact condition, continue with recovering current by reducing front escape, shading and window/TCO absorption, and finish with confirming that the extra current is electrically retained. A cell architecture that increases J_{SC} while weakening FF cannot fully exploit the optical gain potential. An architecture that combines low rear-contact resistance and lower optical loss will surpass the present efficiency level and retain the largest share of the recovered current as terminal power.

The conclusion clarifies what the presented cell sequence does not imply either. First, it does not mean that optical work is of secondary importance, because the largest remaining current-equivalent loss is optical front escape. Second, it does not mean that rear reflector is not important, because the highest efficiency is achieved right after the rear-stack condition change. The proper conclusion is more specific: optical and rear contact conditions should be considered together at the maximum-power point. Rear optical gain has high terminal value if the contact stack retains FF, but if it increases the electrical penalty, the opposite is true.

The proper next step would therefore include p-nc-Si:H rear contact and front-side optical measures that do not affect TCO conduction. The highest impact sequence would be reducing first the front escape, then electrode shading and then TCO/window absorption while checking all along contact resistivity and FF. Such a sequence is a direct consequence of the loss ranking and retention coefficient. It also matches the direction of recent back-contact SHJ developments, where laser patterning, selective contact arrangement, optical thinning and compatible interconnection should be optimized in combination [17,18].

The broader contribution of the analysis lies in the distinction between current recovery and current retention. Current recovery is the optical increase in J_{SC}. Current retention is the share of this increase that survives after including the contact resistance, TCO conductivity, voltage and FF. The 26.81 % SHJ cell demonstrates both values. The former is represented by strong current increase with high retention coefficient. The latter is shown by smaller current increment with lower retention coefficient. Future high-efficiency SHJ studies should report not only the magnitude of the current increase but also how much of it is retained as terminal power.

Thus, the numeric value of the efficiency obtained should be interpreted together with the sequence of operations that resulted in it. The p-nc-Si:H contact enables the electrical

extraction of high currents by lowering contact and series-resistance losses. Then, the front optical condition provides the major current increase. Finally, the MgF_2/Ag rear-stack condition provides the last current increase but also exposes the electrical stack restriction. This is why the former movement is characterized by high retention coefficient, while the latter one is associated with lower retention. This also avoids misinterpretation where the rear reflector is responsible for the whole device gain and the contact is responsible for the current gain.

From the practical side, this study promotes measurement discipline, according to which every optical modification is performed with a simultaneous check of the contact quality. Every change in anti-reflection coatings, TCO thickness, metal fraction, rear reflector or window layer absorption should be accompanied with corresponding FF, series resistance and, if possible, contact resistivity. It is especially important for SHJ cells since their transparent conducting oxides serve simultaneously as optical and electrical layers. The more transparent stack that increases J_{SC} may decrease terminal power by limiting the current spreading and extraction. The present sequence illustrates this point in a measurable way by revealing the difference between $\Gamma = 0.79$ and $\Gamma = 0.24$.

Thus, the final answer of the paper is not merely that p-nc-Si:H is superior to p-a-Si:H or that rear reflector increases current. The answer is that the nanocrystalline hole contact allows changing the operating condition of the cell, enabling it to retain the large fraction of the current gain provided by optical refinement. If such boundary has been established, future optical current increments should be evaluated in terms of their retention. This conclusion is specific to the particular SHJ cell sequence and provides a repeatable methodology for evaluation of future contact-optics combinations in high-efficiency crystalline-silicon solar cells.

Therefore, the central practical conclusion of the paper is precise: added optical current should be regarded as a conditional gain. It becomes valuable if the rear contact, TCO stack and metallization keep the J–V curve power-producing area intact. The 26.81 % cell is successful since the p-nc-Si:H contact satisfies this condition prior to the final optical change.

References

[1] Richter, A.; Hermle, M.; Glunz, S. W. Reassessment of the limiting efficiency for crystalline silicon solar cells. *IEEE Journal of Photovoltaics* **2013**, *3*, 1184–1191. doi:10.1109/JPHOTOV.2013.2270351.

[2] Allen, T. G.; Bullock, J.; Yang, X.; Javey, A.; De Wolf, S. Passivating contacts for crystalline silicon solar cells. *Nature Energy* **2019**, *4*, 914–928. doi:10.1038/s41560-019-0463-6.

[3] De Wolf, S.; Descoeudres, A.; Holman, Z. C.; Ballif, C. High-efficiency silicon heterojunction solar cells: A review. *Green* **2012**, *2*, 7–24. doi:10.1515/green-2011-0018.

[4] Taguchi, M.; Yano, A.; Tohoda, S.; Matsuyama, K.; Maruyama, E. 24.7% record efficiency HIT solar cell on thin silicon wafer. *IEEE Journal of Photovoltaics* **2014**, *4*, 96–99. doi:10.1109/JPHOTOV.2013.2282737.

[5] Yoshikawa, K.; Yoshida, W.; Irie, T.; Kawasaki, H.; Konishi, K.; Ishibashi, H.; Asatani, T.; Adachi, D.; Kanematsu, M.; Uzu, H.; Yamamoto, K. Silicon heterojunction solar cell with interdigitated back contacts for a photoconversion efficiency over 26%. *Nature Energy* **2017**, *2*, 17032. doi:10.1038/nenergy.2017.32.

[6] Qu, X.; et al. Identification of embedded nanotwins at c-Si/a-Si:H interface limiting the performance of high-efficiency silicon heterojunction solar cells. *Nature Energy* **2021**, *6*, 194–202. doi:10.1038/s41560-020-00742-6.

[7] Bivour, M.; Reichel, C.; Hermle, M.; Glunz, S. W. Improving the a-Si:H(p) rear emitter contact of n-type silicon solar cells. *Solar Energy Materials and Solar Cells* **2012**, *106*, 11–16. doi:10.1016/j.solmat.2012.06.031.

[8] Messmer, C.; Bivour, M.; Luderer, C.; Tutsch, L.; Schön, J.; Hermle, M. Influence of interfacial oxides at TCO/doped Si thin film contacts on the charge carrier transport of passivating contacts. *IEEE Journal of Photovoltaics* **2020**, *10*, 343–350. doi:10.1109/JPHOTOV.2019.2957672.

[9] Gogolin, R.; et al. Analysis of series resistance losses in a-Si:H/c-Si heterojunction solar cells. *IEEE Journal of Photovoltaics* **2014**, *4*, 1169–1176. doi:10.1109/JPHOTOV.2014.2323982.

[10] Seif, J. P.; et al. Strategies for doped nanocrystalline silicon integration in silicon heterojunction solar cells. *IEEE Journal of Photovoltaics* **2016**, *6*, 1132–1140. doi:10.1109/JPHOTOV.2016.2571619.

[11] Mazzarella, L.; Kirner, S.; Stannowski, B.; Korte, L.; Rech, B.; Schlatmann, R. p-type microcrystalline silicon oxide emitter for silicon heterojunction solar cells allowing current densities above 40 mA cm^{-2}. *Applied Physics Letters* **2015**, *106*, 023902. doi:10.1063/1.4905906.

[12] Mazzarella, L.; et al. Nanocrystalline silicon emitter optimization for Si-HJ solar cells: Substrate selectivity and CO_2 plasma treatment effect. *Physica Status Solidi A* **2017**, *214*, 1532958. doi:10.1002/pssa.201532958.

[13] Umishio, H.; Sai, H.; Koida, T.; Matsui, T. Nanocrystalline-silicon hole contact layers enabling efficiency improvement of silicon heterojunction solar cells: Impact of nanostructure evolution on solar cell performance. *Progress in Photovoltaics: Research and Applications* **2021**, *29*, 344–356. doi:10.1002/pip.3372.

[14] Fioretti, A. N.; Boccard, M.; Monnard, R.; Ballif, C. Low-temperature p-type microcrystalline silicon as carrier selective contact for silicon heterojunction solar cells. *IEEE Journal of Photovoltaics* **2019**, *9*, 1158–1165. doi:10.1109/JPHOTOV.2019.2919950.

[15] Boccard, M.; Antognini, L.; Paratte, V.; Haschke, J.; Truong, M.; Cattin, J.; Ballif, C. Hole-selective front contact stack enabling 24.1%-efficient silicon heterojunction solar cells. *IEEE Journal of Photovoltaics* **2020**, *11*, 9–15. doi:10.1109/JPHOTOV.2020.3027667.

[16] Lin, H.; Yang, M.; Ru, X.; Wang, G.; Yin, S.; Peng, F.; Hong, C.; Qu, M.; Lu, J.; Fang, L.; Han, C.; Procel, P.; Isabella, O.; Gao, P.; Li, Z.; Xu, X. Silicon heterojunction solar cells with up to 26.81% efficiency achieved by electrically optimized nanocrystalline-silicon hole contact layers. *Nature Energy* **2023**, *8*, 789–799. doi:10.1038/s41560-023-01255-2.

[17] Wang, G.; Su, Q.; Tang, H.; Wu, H.; Lin, H.; Han, C.; Wang, T.; Xue, C.; Lu, J.; Fang, L.; Li, Z.; Xu, X.; Gao, P. 27.09%-efficiency silicon heterojunction back contact solar cell and going beyond. *Nature Communications* **2024**, *15*, 8931. doi:10.1038/s41467-024-53275-5.

[18] Wu, H.; Ye, F.; Yang, M.; Luo, F.; Tang, X.; Tang, Q.; Qiu, H.; Huang, Z.; Wang, G.; Sun, Z.; Lin, H.; Wei, J.; Li, Y.; Tian, X.; Zhang, J.; Xie, L.; Deng, X.; Yuan, T.; Yu, M.; et al. Silicon heterojunction back-contact solar cells by laser patterning. *Nature* **2024**, *635*, 604–609. doi:10.1038/s41586-024-08110-8.

[19] Ru, X.; Yang, M.; Yin, S.; Wang, Y.; Hong, C.; Peng, F.; Yuan, Y.; Sun, C.; Xue, C.; Qu, M.; Wang, J.; Lu, J.; Fang, L.; Deng, H.; Xie, T.; Liu, S. F.; Li, Z.; Xu, X. Silicon heterojunction solar cells achieving 26.6% efficiency on commercial-size p-type silicon wafer. *Joule* **2024**, *8*, 1092–1104. doi:10.1016/j.joule.2024.01.015.

[20] Zhang, Y.; Shi, T.; Duan, L.; Hoex, B.; Tang, Z. Progress in passivating selective contacts for heterojunction silicon solar cells. *Nano Energy* **2024**, *131*, 110282. doi:10.1016/j.nanoen.2024.110282.

[21] Yablonovitch, E. Statistical ray optics. *Journal of the Optical Society of America* **1982**, *72*, 899–907. doi:10.1364/JOSA.72.000899.

[22] Green, M. A. Self-consistent optical parameters of intrinsic silicon at 300 K including temperature coefficients. *Solar Energy Materials and Solar Cells* **2008**, *92*, 1305–1310. doi:10.1016/j.solmat.2008.06.009.

[23] Holman, Z. C.; Descoeudres, A.; Barraud, L.; Fernandez, F. Z.; Seif, J. P.; De Wolf, S.; Ballif, C. Current losses at the front of silicon heterojunction solar cells. *IEEE Journal of Photovoltaics* **2012**, *2*, 7–15. doi:10.1109/JPHOTOV.2011.2174967.

[24] Han, C.; et al. Towards bifacial silicon heterojunction solar cells with reduced TCO use. *Progress in Photovoltaics: Research and Applications* **2022**, *30*, 750–762. doi:10.1002/pip.3541.

[25] Richter, A.; Glunz, S. W.; Werner, F.; Schmidt, J.; Cuevas, A. Improved quantitative description of Auger recombination in crystalline silicon. *Physical Review B* **2012**, *86*, 165202. doi:10.1103/PhysRevB.86.165202.

[26] Cox, R. H.; Strack, H. Ohmic contacts for GaAs devices. *Solid-State Electronics* **1967**, *10*, 1213–1218. doi:10.1016/0038-1101(67)90063-9.

[27] Reeves, G. K.; Harrison, H. B. Obtaining the specific contact resistance from transmission line model measurements. *IEEE Electron Device Letters* **1982**, *3*, 111–113. doi:10.1109/EDL.1982.25502.

[28] Pysch, D.; Mette, A.; Glunz, S. W. A review and comparison of different methods to determine the series resistance of solar cells. *Solar Energy Materials and Solar Cells* **2007**, *91*, 1698–1706. doi:10.1016/j.solmat.2007.05.026.

[29] Brendel, R.; Peibst, R. Contact selectivity and efficiency in crystalline silicon photovoltaics. *IEEE Journal of Photovoltaics* **2016**, *6*, 1413–1420. doi:10.1109/JPHOTOV.2016.2598267.

[30] Sharma, M.; Panigrahi, J.; Komarala, V. K. Nanocrystalline silicon thin-film growth and application for silicon heterojunction solar cells: A short review. *Nanoscale Advances* **2021**, *3*, 3373–3383. doi:10.1039/D1NA00188D.

[31] Zhao, Y.; et al. Doped hydrogenated nanocrystalline silicon oxide layers for high-efficiency c-Si heterojunction solar cells. *Progress in Photovoltaics: Research and Applications* **2020**, *28*, 425–435. doi:10.1002/pip.3264.